

# GW150914: spin-based constraints on the merger time of the progenitor system

Doron Kushnir,<sup>1,2\*</sup> Matias Zaldarriaga,<sup>1</sup> Juna A. Kollmeier<sup>1,3</sup> and Roni Waldman<sup>4</sup>

<sup>1</sup>*School of Natural Sciences, Institute for Advanced Study, Princeton, NJ, 08540, USA*

<sup>2</sup>*John N. Bahcall Fellow*

<sup>3</sup>*Observatories of the Carnegie Institution of Washington, 813 Santa Barbara Street, Pasadena, CA 91101, USA*

<sup>4</sup>*Racah Institute of Physics, Hebrew University, Jerusalem, 9190401, Israel*

Accepted XXX. Received YYY; in original form ZZZ

## ABSTRACT

We explore the implications of the observed low spin of GW150914 within the context of stellar astrophysics and progenitor models. We conclude that many of the recently proposed scenarios are in marked tension with this observation. We derive a simple model for the observed spin in the case that the progenitor system was a field binary composed of a black hole (BH) and a Wolf–Rayet star and explore the implications of the observed spin for this model. The spin observation allows us to place a lower limit for the delay time between the formation of the BH+BH binary and the actual merger,  $t_{\text{merge}}$ . We use typical values for these systems to derive  $t_{\text{merge}} \gtrsim 10^8$  yr, which proves to be an important diagnostic for different progenitor models. We anticipate the next series of events, and the associated spin parameters, will ultimately yield critical constraints on formation scenarios and on stellar parameters describing the late-stage evolution of massive stars.

**Key words:** gravitational waves – binaries: close – stars: Wolf–Rayet

## 1 INTRODUCTION

The era of gravitational wave astronomy has arrived. Both the strength of the signal in GW150914, as well as its form, were a striking revelation to all (Abbott et al. 2016). In particular, the reported masses of the system – consistent with a black hole+black hole (BH+BH) binary merger with estimated BH masses<sup>1</sup> of  $M_1 = 35.7^{+5.4}_{-3.8} \pm 1.1$ ,  $M_2 = 29.1^{+3.8}_{-4.4} \pm 0.2$  — are significantly ‘heavier’ than expected based on the known mass function of stellar mass BHs within the Milky Way. The delightfully unexpected properties of GW150914 have unleashed the creative fury of the theoretical astrophysics community. As a result, there is an enormous range of proposed channels all aiming to produce BHs in the observed mass range.

In this article, we explore another property of GW150914 — its observed (low) spin. The effective inspiral spin parameter,

$$\chi_{\text{eff}} = \frac{M_1 \vec{a}_1 + M_2 \vec{a}_2}{M_1 + M_2} \cdot \hat{L} \quad (1)$$

(where  $\vec{a}_1$  and  $\vec{a}_2$  are the dimensionless BH spins,  $\vec{a} =$

$c\vec{S}/GM^2$ , and  $\hat{L}$  is the direction of orbital angular momentum), is observed to be  $\chi_{\text{eff}} = -0.06^{+0.17}_{-0.18} \pm 0.01$ .

There are multiple proposed channels for the merger of stellar-mass BHs including, but not limited to isolated stellar field binary merger (hereafter, the *classical scenario*, Phinney 1991; Tutukov & Yungelson 1993; Belczynski et al. 2016), dynamical formation in dense environments (e.g. in globular clusters, Sigurdsson & Hernquist 1993), and merger inside a massive star envelope (Fryer et al. 2001; Reisswig et al. 2013; Loeb 2016; Woosley 2016). Recently, an isolated stellar field binary scenario that includes chemically homogeneous stars has been discussed by Mandel & de Mink (2016); Marchant et al. (2016), and de Mink & Mandel (2016). For a more complete reference list of proposed channels, see Abbott et al. (2016). Some of these scenarios predict alignment of the BH spin and the orbital angular momentum. In this case  $\chi_{\text{eff}}$  is just the mass-weighted mean of the dimensionless spins  $a = c|\vec{S}|/GM^2$ , which can generically be quite large in possible tension with the observed low  $\chi_{\text{eff}}$ . Following are the examples.

(i) Formation inside a massive star envelope: the fission of the core to two BHs should generally lead to  $a \sim 1$  for each of them. For example, Reisswig et al. (2013) simulate the fission to two BHs within a common envelope and the subsequent BH–BH merger. In the final orbits before the

\* E-mail: kushnir@ias.edu

<sup>1</sup> The error quotes both the 90% credible interval and an estimate for the 90% range of systematic error (Abbott et al. 2016).

merger, each simulated BH has  $a \approx 0.7$ , which would lead to  $\chi_{\text{eff}} \approx 0.7$  compared to the low observed value  $\chi_{\text{eff}} \ll 1$ .

(ii) The chemically homogeneous stars scenario: Yoon et al. (2006) derived the condition  $v_{\text{eq}} \geq 0.2\sqrt{GM/R}$ , where  $v_{\text{eq}} = R\Omega$  is the equatorial velocity at the stellar radius,  $R$ , and  $\Omega$  is the angular spin velocity of the star, as the threshold for homogenous evolution (see their fig. 3; larger  $v_{\text{eq}}$  are required for lower mass stars). Neglecting the effect of mass-loss during the collapse of a fully mixed star to a BH (which is justified later on), the dimensionless spin of the BH satisfies:

$$\begin{aligned} a &\geq 0.2cr_g^2\sqrt{\frac{R}{GM}} \\ &\approx 2.7\left(\frac{r_g^2}{0.075}\right)\left(\frac{R}{2R_\odot}\right)^{1/2}\left(\frac{M}{30M_\odot}\right)^{-1/2}, \end{aligned} \quad (2)$$

where  $r_g^2$  is the (dimensionless) radius of gyration of the star related to the moment of inertia by  $I = r_g^2R^2M$ . Equation (2) implies that both BHs should have close-to-maximal spins ( $a \approx 1$ ). This prediction of  $\chi_{\text{eff}} \approx 1$  is thus in seeming tension with the low observed value  $\chi_{\text{eff}} \ll 1$ . In a more recent study of homogenous evolution, Marchant et al. (2016) provide the threshold  $a$  values for their models directly. All systems with  $M_1 + M_2 \lesssim 100M_\odot$  that merge within Hubble time satisfy  $a \gtrsim 0.5$  for both components, leading to  $\chi_{\text{eff}} \gtrsim 0.5$ , which also in tension with the low observed value  $\chi_{\text{eff}} \ll 1$ .

(iii) Perna et al. (2016) suggested that a disc forms around one of the BHs to later power a short gamma-ray burst. For the specific scenario that they proposed, the spin of this BH is  $a \approx 1$ , which is also in tension with the low observed value  $\chi_{\text{eff}} \ll 1$  for GW150914. Note, however, that by modifying the angular momentum profile of the BH progenitor, this scenario can be tuned to produce a BH with a low spin.

These models, in their raw form, generally predict  $\chi_{\text{eff}}$  close to unity. The observation in GW150914 of  $\chi_{\text{eff}} \ll 1$  thus already provides some constraining power on the details of these models.

In this paper, we will analyse the *classical scenario* and show that the spin observation allows us to place a lower limit on the delay time between the formation of the BH+BH binary and the actual merger,  $t_{\text{merge}}$ . This arises because a short delay time corresponds to small separation between the primary BH and the star that evolves to become the second BH. For small separations, the primary BH applies torque to the star, spinning it towards synchronization. The angular momentum resulting from this process violates the observed upper limit given by the observed  $\chi_{\text{eff}}$ . We derive a simple model to describe this process, and we elucidate the basic considerations here so that future events may be similarly used to constrain models. We use typical values for these systems to derive for GW150914  $t_{\text{merge}} \gtrsim 10^8$  yr.

Our paper is organized as follows. In Section 2 we consider the angular momentum evolution of the secondary star as it collapses to a BH, examining the competing effects of wind-losses and torque-gains. In Section 3 we consider the allowed range of scenarios and demonstrate the application of our limits. In Section 4, we consider the caveats and limitations to our main argument. We conclude in Section 5.

## 2 ANGULAR MOMENTUM EVOLUTION IN A ‘CLASSIC’ SCENARIO

The *classical scenario* for the merger of stellar-mass BHs from an isolated stellar field binary was worked out nearly three decades ago with subsequent modern improvements (Phinney 1991; Tutukov & Yungelson 1993; Belczynski et al. 2016). In this picture, prior to the collapse of the second BH, the progenitor system is an isolated stellar field binary that is composed of a Wolf-Rayet (WR) star with a mass  $M$  and a BH with a mass  $M/q$ ,  $q$  being defined as the mass ratio.

We now investigate the angular momentum evolution of the WR star. The final angular momentum of the WR star is the angular momentum of the second BH under the assumption that there is no mass-loss during the collapse. Mass-loss also increases the initial semi-major axis of the BH+BH orbit compared with the BH+WR orbit. We will revisit this assumption in Section 5 and show that mass-loss during the collapse does not change our result significantly. We further assume that the kick velocity of the second BH at birth is very small compared with the orbital velocity. Any scenario involving a large BH natal kick is ruled out by the existence of the merger.

For an initial orbital semi major axis,  $d$ , we can normalize the dimensionless spin of the star,  $a$ , to the orbital angular velocity,  $\omega = \sqrt{G(M+M/q)/d^3}$ :

$$\begin{aligned} a &= \frac{cJ}{GM^2} = \frac{cr_g^2R^2}{GM} \left(\frac{1+q}{2q}\right)^{1/2} \left(\frac{2GM}{d^3}\right)^{1/2} \frac{\Omega}{\omega} \\ &\equiv a_{\text{sync}} \frac{\Omega}{\omega}. \end{aligned} \quad (3)$$

For synchronization between the stellar spin and the orbit ( $\Omega = \omega$ ), we define  $a = a_{\text{sync}}$ .

Because the merger time due to gravitational wave emission,  $t_{\text{merge}}$ , also depends simply on the initial orbital properties and component masses (Peters 1964):

$$t_{\text{merge}} = \frac{5}{512} \frac{c^5}{G^3 M^3} \frac{2q^2}{1+q} d^4, \quad (4)$$

we can write  $a_{\text{sync}}$  as follows:

$$\begin{aligned} a_{\text{sync}} &\approx 0.44 \left(\frac{q^2(1+q)}{2}\right)^{1/8} \left(\frac{r_g^2}{0.075}\right) \left(\frac{R}{2R_\odot}\right)^2 \times \\ &\quad \left(\frac{M}{30M_\odot}\right)^{-13/8} \left(\frac{t_{\text{merge}}}{1\text{Gyr}}\right)^{-3/8}. \end{aligned} \quad (5)$$

Although not used later on, it may be useful for subsequent studies to derive similar expression for the initial orbital

period, equatorial velocity, and the break-up fraction:

$$\begin{aligned}
 P &\approx 1.81 \left( \frac{q^2(1+q)}{2} \right)^{-1/8} \left( \frac{M}{30M_\odot} \right)^{5/8} \left( \frac{t_{\text{merge}}}{1 \text{ Gyr}} \right)^{3/8} \text{ day}, \\
 v_{\text{eq}} &= R\Omega = R \left( \frac{1+q}{2q} \right)^{1/2} \left( \frac{2GM}{d^3} \right)^{1/2} \frac{\Omega}{\omega} \\
 &\approx 55.8 \left( \frac{q^2(1+q)}{2} \right)^{1/8} \left( \frac{R}{2R_\odot} \right) \times \\
 &\quad \left( \frac{M}{30M_\odot} \right)^{-5/8} \left( \frac{t_{\text{merge}}}{1 \text{ Gyr}} \right)^{-3/8} \frac{\Omega}{\omega} \text{ km s}^{-1}, \\
 f_{\text{break}} &= \frac{\Omega^2 R^3}{GM} = 2 \left( \frac{R}{d} \right)^3 \left( \frac{1+q}{2q} \right) \left( \frac{\Omega}{\omega} \right)^2 \\
 &\approx 1.09 \cdot 10^{-3} \left( \frac{q^2(1+q)}{2} \right)^{1/4} \left( \frac{R}{2R_\odot} \right)^3 \times \\
 &\quad \left( \frac{M}{30M_\odot} \right)^{-9/4} \left( \frac{t_{\text{merge}}}{1 \text{ Gyr}} \right)^{-3/4} \left( \frac{\Omega}{\omega} \right)^2. \tag{6}
 \end{aligned}$$

The angular momentum evolution of the WR star is determined by two competing processes. Stellar winds decrease the angular momentum of the star (Section 2.1), while torque applied to the star by the BH increases the angular momentum, driving it towards  $a_{\text{sync}}$  (Section 2.2). We now investigate the impact of each of these processes on the total angular momentum evolution.

## 2.1 Wind Losses

Mass-loss from WR stars is complicated theoretically and observationally, thus the estimated rates are highly uncertain. A typical estimate is  $\approx 10^{-5} M_\odot \text{ yr}^{-1}$  (see Crowther 2007, and references therein), while Nugis & Lamers (2000) estimate  $M/\dot{M} \approx 10^6 \text{ yr}$  independent of mass. An expected dependence of the mass-loss rate on metallicity further complicates the estimates (Vink et al. 2001). Here, we assume that over the time of the WR phase,  $t_{\text{WR}}$ , the star does not lose a significant fraction of its mass, i.e.  $t_{\text{WR}} \lesssim M/\dot{M}$ . For massive  $\gtrsim 10M_\odot$  WR stars, this is a reasonable assumption, as the estimated lifetime is  $t_{\text{WR}} \approx 3 \cdot 10^5 \text{ yr}$  (see ?, for a recent study), and  $M/\dot{M} \gtrsim 10^6 \text{ yr}$ . We are interested in  $t_{\text{wind}}$ , the time-scale for loss of angular momentum resulting from winds. For  $t_{\text{wind}} \lesssim t_{\text{WR}}$  the angular momentum is exponentially suppressed due to the wind. We now estimate this time-scale for the system of interest.

Assuming the stellar radius is constant during the mass loss and that the mass is lost from a spherical shell at the stellar surface (see discussion in Ro & Matzner 2016), we can write the rate of angular momentum loss as follows (Packet 1981):

$$\dot{J} = \dot{I}\Omega = \frac{2\dot{M}R^2\Omega}{3}. \tag{7}$$

We can estimate  $t_{\text{wind}}$  by taking the ratio between  $J$  and  $\dot{J}$ ,

$$t_{\text{wind}} \equiv \frac{a}{\dot{a}} \approx \frac{J}{\dot{J}} \approx \frac{3}{2} \frac{r_g^2 M}{t_g^2 \dot{M}} \approx 0.1 \left( \frac{r_g^2}{0.075} \right) \frac{M}{\dot{M}}, \tag{8}$$

which suggests  $t_{\text{wind}} \gtrsim 10^5 \text{ yr}$ . In the case that the wind is magnetized, the specific angular momentum of the wind is larger than the previous estimate by a factor  $R_A/R$ , where

$R_A$  is the Alfvén radius, which can significantly decrease the value of  $t_{\text{wind}}$ .

We can use the observed rotational periods of isolated WR stars to estimate  $t_{\text{wind}}$ . There are a few WR stars with a claimed detection of rotation. Two of them show no signs of a companion and quite high angular spin velocities; WR 134 with  $\Omega \approx 2.7 \text{ day}^{-1}$  (McCandliss et al. 1994; Morel et al. 1999) and WR 6 with  $\Omega \approx 1.7 \text{ day}^{-1}$  (St-Louis et al. 1995; Morel et al. 1997). Assume that in the beginning of the WR phase ( $t=0$ ), the break-up fraction at the surface was  $f$ , and that the star loses angular momentum only by the wind, then the angular spin velocity is given by

$$\begin{aligned}
 \Omega(t) &= \sqrt{\frac{GMf}{R^3}} \exp(-t/t_{\text{wind}}) \\
 \Rightarrow t_{\text{wind}} &= \frac{t}{\ln \left( \frac{\sqrt{GMf}}{R^3 \Omega^2} \right)}. \tag{9}
 \end{aligned}$$

The factor in the denominator is 2–3 for the observed  $\Omega$  values, typical  $R$  and  $M$  values, and  $f=0.01$ . Therefore, in the case that the age of WR 134 and WR 6 is some significant fraction of  $t_{\text{WR}}$ , we can estimate  $t_{\text{wind}} \sim 10^5 \text{ yr}$ . Another possibility is that these stars are very young and this is the reason they are observed to be rotating fast. In this case  $t_{\text{wind}}$  is smaller by a factor of  $t/t_{\text{WR}}$ .

## 2.2 Torque Gains

The torque applied to a star in a binary system was first calculated by Zahn (1975). We use the following expression for the torque applied to the star by the BH, as further described in Kushnir (2016b)<sup>2</sup>:

$$\tau \approx \frac{G(M/q)^2}{r_c} \left( \frac{r_c}{d} \right)^6 \left[ \frac{4(\omega - \Omega)^2 r_c^3}{GM_c} \right]^{4/3} \frac{\rho_c}{\bar{\rho}_c} \left( 1 - \frac{\rho_c}{\bar{\rho}_c} \right)^2, \tag{11}$$

where  $\rho$  is the density,  $\bar{\rho}$  is the mean density inside the sphere of radius  $r$ , and the subscript  $c$  indicates values at the convective core boundary. Given this expression for the torque, the change in  $a$  can be computed:

$$\dot{a} = \frac{c}{GM^2} \tau \equiv \frac{a_{\text{sync}}}{t_\tau} \left| 1 - \frac{a}{a_{\text{sync}}} \right|^{8/3}, \tag{12}$$

<sup>2</sup> In our case we can assume that the normalized apparent frequency of the tide,  $s = 2|\omega - \Omega| \sqrt{R^3/GM}$ , satisfies  $s^{-1} \gg 1$ :

$$\begin{aligned}
 s &< 2\omega \left( \frac{R^3}{GM} \right)^{1/2} = 2^{3/2} \left( \frac{1+q}{2q} \right)^{1/2} \left( \frac{R}{d} \right)^{3/2}, \\
 \Rightarrow s^{-1} &\gtrsim 15.2 \left( \frac{q^2(1+q)}{2} \right)^{-1/8} \left( \frac{R}{2R_\odot} \right)^{-3/2} \\
 &\quad \times \left( \frac{t_{\text{merge}}}{\text{Gyr}} \right)^{3/8} \left( \frac{M}{30M_\odot} \right)^{9/8}. \tag{10}
 \end{aligned}$$

In this case, the forced oscillations in the envelope behave like a purely travelling wave. For the case that  $s^{-1}$  is small compared with unity, one must further consider the damping of the waves in the envelope, which is not the relevant regime and thus outside the scope of this paper.

where the relevant time-scale is

$$\begin{aligned}
 t_\tau &= a_{\text{sync}} \frac{GM^2}{c\tau(\Omega=0)} \\
 &= 2^{-21/6} \left(\frac{512}{5}\right)^{17/8} q^{-1/8} \left(\frac{1+q}{2q}\right)^{31/24} r_g^2 \left(\frac{R}{r_c}\right)^2 \\
 &\times \left(\frac{GM}{r_c c^2}\right)^{109/24} \left(\frac{GM_c}{r_c c^2}\right)^{4/3} \left(\frac{\rho_c}{\bar{\rho}_c}\right)^{-1} \left(1 - \frac{\rho_c}{\bar{\rho}_c}\right)^{-2} \\
 &\times \left(\frac{ct_{\text{merge}}}{r_c}\right)^{9/8} t_{\text{merge}} \\
 &\equiv q^{-1/8} \left(\frac{1+q}{2q}\right)^{31/24} f_\tau(t_{\text{merge}}) t_{\text{merge}} \quad (13)
 \end{aligned}$$

In order to estimate this time-scale, we require knowledge of the physical structure ( $R$ ,  $r_c$ ,  $M_c$ ,  $r_g^2$ ) of the WR star. The time-scale is especially sensitive to  $r_c$  as it scales with  $r_c^{-9}$ , and much less sensitive to the other parameters. Note that  $t_\tau$  scales as  $t_{\text{merge}}^{17/8}$ , and since we are interested in estimating  $t_{\text{merge}}$  to an order of a magnitude, it is sufficient to estimate  $f_\tau$  (at some fixed  $t_{\text{merge}}$ ) to factor of a few, which we presently evaluate.

### 2.3 WR stellar models

The values of  $R$ ,  $r_c$ ,  $M_c$ , and  $r_g^2$  are challenging to directly observe, due to optically thick stellar winds that obscure the stellar surface, making the interpretation of measurements challenging. It is therefore uncertain to use empirical estimates of these quantities, and we are forced to rely on stellar evolution models to obtain estimates of these parameters.

We construct stellar evolution models using the publicly available package MESA version 6596 (Paxton et al. 2011, 2013, 2015). We aim to cover a wide range of masses during the WR phase ( $\approx [5, 32]M_\odot$ ), and for that we select from a set of models having zero-age main sequence masses in the range  $[40, 100]M_\odot$ , metallicities between  $[0.01, 1]Z_\odot$ , and initial rotation between  $[0.4, 0.6]$  of breakup. We use the WR model profiles during the epoch where the time to core-collapse is greater than  $10^4$  yr and the stellar radius is smaller than  $2R_{\text{SM}}$ , where  $R_{\text{SM}}$  is the WR radius according to Schaerer & Maeder (1992).

In all models, mass-loss was determined according to the ‘Dutch’ recipe in MESA, combining the rates from Glebbeek et al. (2009); Nieuwenhuijzen & de Jager (1990); Nugis & Lamers (2000), and Vink et al. (2001), with a coefficient  $\eta = 1$ , convection according to the Ledoux criterion, with mixing length parameter  $\alpha_{\text{mlt}} = 2$ , semi-convection efficiency parameter  $\alpha_{\text{sc}} = 0.1$  (Paxton et al. 2013, equation 12), and exponential overshoot parameter  $f = 0.008$  (Paxton et al. 2011, equation 2). For the atmosphere boundary condition we use the simple option of MESA (Paxton et al. 2011, eq. 3).

In Figure 1, we present  $R$  and  $r_c$  as a function of  $M$  for the models we consider. Our results can be fit as  $\log_{10}(R/R_\odot) \approx -0.70 + 0.70 \log_{10}(M/M_\odot)$  and as  $\log_{10}(r_c/R_\odot) \approx -1.25 + 0.75 \log_{10}(M/M_\odot)$ . The profiles are well described by polytropes with  $n \approx 2.5$ – $3.5$  and  $r_g^2$  is in the range  $\approx 0.05$ – $0.09$ , which roughly corresponds to these polytropes. Our calculated stellar radii are compared with the stellar evolution models of Schaller et al. (1992),

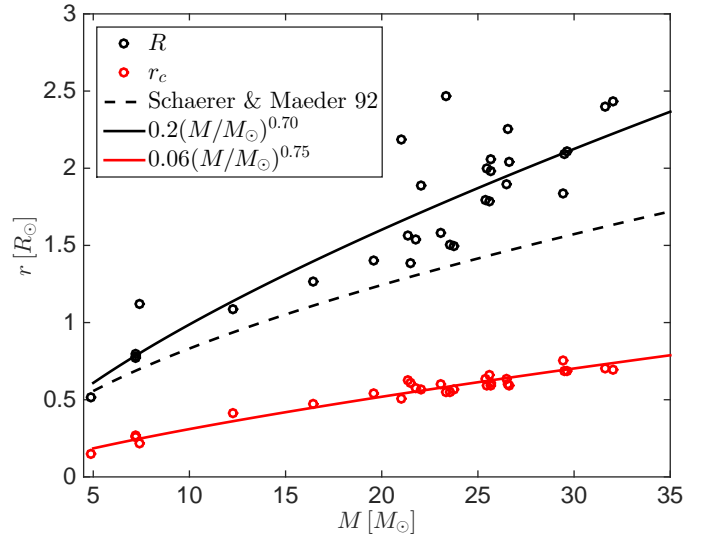


**Figure 1.**  $R$  (black curves) and  $r_c$  (red curves) for a series of stellar models. The open symbols show our results for a series of models computed by MESA. Simple fits to these points are shown by the solid black and red curves. The dashed black curve shows the estimate of  $R$  from Schaerer & Maeder (1992) based on the stellar evolution models of Schaller et al. (1992). The predicted larger radii ( $\sim 30\%$ ) at fixed mass in our models relative to the Schaller et al. (1992) models, likely due to our simplified treatment of the stellar atmosphere, do not significantly impact our final results.

evaluated in Schaerer & Maeder (1992). We predict larger radii ( $\sim 30\%$ ) at fixed mass in our models relative to the Schaller et al. (1992), possibly because of the simple MESA photosphere boundary condition that we used (see discussion in Ro & Matzner 2016). We note that generally, stellar evolution models predict radii that are significantly smaller than those derived from atmospheric models ( $\approx 3R_\odot$  in some cases; see Crowther 2007, and references therein), and therefore should be considered at the moment as a rough estimate. Nevertheless, the uncertainty in the stellar radii is insignificant for our final results, which depend much more strongly on the core radii.

Instead of fitting separately for each parameter, we directly calculate, for each WR model,  $f_\tau(1\text{Gyr})$  from Equation (13). The results are presented in Figure 2. The main uncertainty in the value of  $f_\tau$  is the core radius  $r_c$ , as  $f_\tau \propto r_c^{-9}$ . The scatter of  $f_\tau$  at fixed mass is completely driven by the scatter of  $r_c$  in Figure 1. We approximate  $f_\tau(1\text{Gyr}) \approx 0.01$ , which reproduces the numerical results to better than a factor of 3, as demonstrated by the shaded band in Figure 2. This allows us to rewrite Equation (13) simply as

$$t_\tau \approx 10^7 q^{-1/8} \left(\frac{1+q}{2q}\right)^{31/24} \left(\frac{t_{\text{merge}}}{1\text{Gyr}}\right)^{17/8} \text{yr}. \quad (14)$$

We are now able to evaluate the angular momentum evolution of the system prior to merger.

### 3 IMPLICATIONS

At the beginning of the WR phase, we expect  $0 \leq a \leq a_{\text{sync}}$ . That is, following the previous evolution phases of the sys-

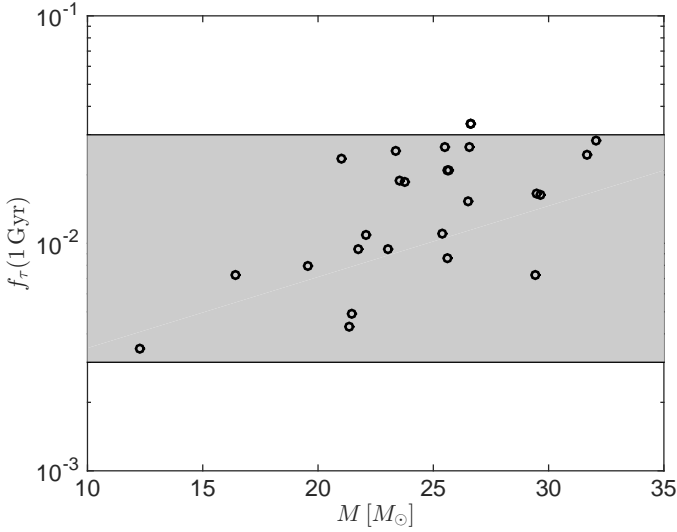


**Figure 2.** The pre-factor from Equation (13),  $f_\tau(1\text{Gyr})$ , as function of the stellar mass. The main uncertainty in the value of  $f_\tau$  is the core radius  $r_c$ , as  $f_\tau \propto r_c^{-9}$ . The scatter of  $f_\tau$  at fixed mass is completely driven by the scatter of  $r_c$  in Figure 1. We approximate  $f_\tau(1\text{Gyr}) \approx 0.01$ , which reproduces the numerical results to better than a factor of 3, as demonstrated by the shaded band.

tem, we neither expect the star to be spinning faster than the synchronization value nor retrograde. We can therefore compute the evolution of the spin taking into account the breaking and torquing described above. Including both effects, the evolution of  $a$  is simply

$$\dot{a} = \frac{a_{\text{sync}}}{t_\tau} \left(1 - \frac{a}{a_{\text{sync}}}\right)^{8/3} - \frac{a}{t_{\text{wind}}}. \quad (15)$$

We can integrate Equation (15) directly to find  $a(t_{\text{WR}})$  given  $t_{\text{WR}}$ ,  $t_{\text{wind}}$ ,  $t_\tau$ , and  $a(0)$ . The angular momentum of the second BH is given by  $\min(a(t_{\text{WR}}), 1)$ . We can gain some insight into the solution of Equation (15) by writing it as

$$x' = \frac{t_{\text{wind}}}{t_\tau} (1-x)^{8/3} - x, \quad (16)$$

where  $x = a/a_{\text{sync}}$ , prime indicated a derivative with respect to  $t/t_{\text{wind}}$ , and  $0 \leq x(0) \leq 1$ . For large enough  $t_{\text{WR}}/t_{\text{wind}}$  we have  $x(t_{\text{WR}}/t_{\text{wind}}) \approx x_{\text{eq}}$ , where

$$\frac{t_{\text{wind}}}{t_\tau} (1-x_{\text{eq}})^{8/3} = x_{\text{eq}}. \quad (17)$$

The solution of Equation (16) in a few representative cases can be approximated as follows.

- (i)  $t_{\text{wind}} \gtrsim t_{\text{WR}}$ ,  $x(0) = 1$ ;  $x(t_{\text{WR}}/t_{\text{wind}}) \approx \max(1 - t_{\text{WR}}/t_{\text{wind}}, x_{\text{eq}})$ .
- (ii)  $t_{\text{wind}} \gtrsim t_{\text{WR}}$ ,  $x(0) = 0$ ;  $x(t_{\text{WR}}/t_{\text{wind}}) \approx \min(t_{\text{WR}}/t_\tau, x_{\text{eq}})$ .
- (iii)  $t_{\text{wind}} \lesssim t_{\text{WR}}$ ,  $x(0) = 1$ ;  $x(t_{\text{WR}}/t_{\text{wind}}) \approx \max[\exp(-(t_{\text{WR}}/t_{\text{wind}})), x_{\text{eq}}]$ .
- (iv)  $t_{\text{wind}} \lesssim t_{\text{WR}}$ ,  $x(0) = 0$ ;  $x(t_{\text{WR}}/t_{\text{wind}}) \approx x_{\text{eq}}$ .

We solve Equation (15) for four representative examples and show the results in Figure 3. We consider cases when  $t_{\text{wind}} \gtrsim t_{\text{WR}}$  or  $t_{\text{wind}} \lesssim t_{\text{WR}}$  and when the initial spin is close to zero or close to  $a_{\text{sync}}$ . In our examples for Figure 3 we

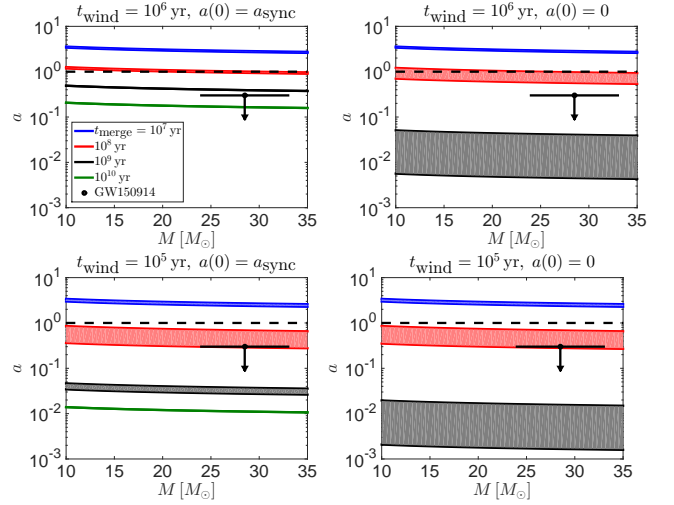


**Figure 3.** (a)–(d) Dimensionless spin-parameter of the secondary BH as a function of  $M$  for different limiting cases. The black symbol shows GW150914. Blue, red, black, and green lines show merger times of  $10^7$ ,  $10^8$ ,  $10^9$ , and  $10^{10}$  yr. The shaded band for each merger time represent the range  $3 \cdot 10^{-3} \leq f_\tau(1\text{Gyr}) \leq 3 \cdot 10^{-2}$ , which corresponds to the uncertainty in its value (shaded band in Figure 2). Lower values of  $a$  correspond to higher values of  $f_\tau$ . We choose  $t_{\text{WR}}/t_{\text{wind}} = 0.3$  (upper panels) and  $t_{\text{WR}}/t_{\text{wind}} = 3$  (lower panels) to span reasonable parameters for the wind. We study cases when the initial spin is close to zero (right-hand panels) or close to  $a_{\text{sync}}$  (left-hand panels). For convenience, we plot values above the  $a = 1$  limit (dashed line).

choose  $t_{\text{WR}}/t_{\text{wind}} = 0.3$  ( $t_{\text{wind}} = 10^6$  yr) and  $t_{\text{WR}}/t_{\text{wind}} = 3$  ( $t_{\text{wind}} = 10^5$  yr) so as to span reasonable parameters for the wind. We calculated for both  $f_\tau(1\text{Gyr}) = 3 \cdot 10^{-3}$  and  $f_\tau(1\text{Gyr}) = 3 \cdot 10^{-2}$ , to span the uncertainty in its value. We further assume that  $q = 1$ , consistent with GW150914. Our results are compared with the limit from GW150914,  $a < 0.3$  at 90% probability (Abbott et al. 2016). In our comparison, we use the values for the less massive BH as the more massive BH yields slightly stronger constraints. We conclude that in order for  $a$  not to exceed the observed limit, we must have  $t_{\text{merge}} \gtrsim 10^8$  yr. This lower limit is driven by the cases with small  $t_{\text{wind}}$ , and is independent of the value of  $a(0)$ . Smaller values of  $t_{\text{wind}}$  would decrease the derived lower limit. For  $t_{\text{wind}} = 10^4$  yr, we obtained  $t_{\text{merge}} \gtrsim \text{few} \times 10^7$  yr. Models of the classical scenario can be compared with the derived lower limit of  $t_{\text{merge}}$ . For example, the vast majority of models in Belczynski et al. (2016) fulfil this condition. Note that the scenario of no winds and  $a(0) = a_{\text{sync}}$  is not far from being ruled out, as using the age of the Universe for  $t_{\text{merge}}$  in Equation (3) leads in this case to  $a = a_{\text{sync}} \approx 0.15$ .

#### 4 CAVEATS

We assume there is no mass-loss during the collapse. Mass-loss changes our analysis in two ways. First, mass-loss widens the initial separation of the BH+BH orbit compared with the BH+WR orbit. This effect makes the merger time longer, which does not affect the derived lower limit for  $t_{\text{merge}}$ . Secondly, angular momentum is lost with the mass ejection, which may change our estimate for the spin evolution of the BH. We estimate the possible decrease in  $a$  by

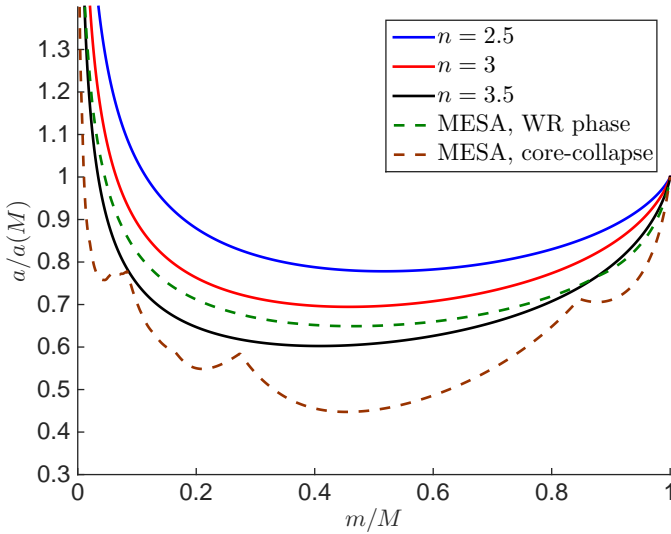


**Figure 4.** Effect of mass-loss on angular momentum evolution. We compute the change in  $a$  for three different polytropes in solid-body rotation as mass is changed relative to an initial mass (solid). We compare the polytrope estimate to one of our MESA models with a WR mass of  $M \approx 30M_{\odot}$  for both the WR phase prior to the last burning stages (dashed green) and for the time of core-collapse (dashed brown), which demonstrate the robustness of the polytrope estimates. The possible decrease in  $a$  is modest (20–50%), and obtained for substantial mass-loss.

considering in Figure 4 polytropes with solid body rotation, which is the expected configuration during the WR phase. The very last burning stages of the WR star prior to collapse are expected to be sufficiently fast, such that angular momentum transfer can be neglected and each mass shell retains its original  $a$  value. We compare the polytrope estimate to one of our MESA models with a WR mass of  $M \approx 30M_{\odot}$  for both the WR phase prior to the last burning stages and for the time of core-collapse, which demonstrate the robustness of the polytrope estimates. We show in Figure 4 that the value of  $a$  can decrease by 20–50% for a large mass ejection, which does not significantly affect our analysis. Moreover, if indeed the collapse was accompanied by a supernova, then it should be a Type Ibc supernova, for which the mass of the ejecta is small compared to  $30M_{\odot}$  (e.g., Lyman et al. 2016). Indeed, such a system is an expected outcome of a Type Ibc supernova for collapse-induced thermonuclear explosions (Kushnir 2015a,b).

We thus conclude that our analysis is robust to the simplifications we have made.

## 5 DISCUSSION

We have provided a simple framework for using the observed (low) BH spin of GW150914 to constrain the BH merger time and thus the characteristics of the progenitor system. We have shown that already with a single event, the observed constraint on  $\chi_{\text{eff}}$  comes astonishingly close to ruling out certain scenarios. Future events will allow us to map the true delay-time distribution as a function of progenitor mass – a critical quantity in understanding the latest-stage evolution of the progenitors — for comparison with predictions. We

eagerly await the results of future observations of gravity waves from these truly remarkable events and expect that the measurement of the spins will be very informative to constrain the different formation channels that have been proposed.

## ACKNOWLEDGEMENTS

We thank Ben Bar-Or, Jeremy Goodman, Boaz Katz, Roman Rafikov, and Eli Waxman for discussions. MZ is supported in part by the NSF grants PHY-1213563, AST-1409709, and PHY-1521097. JAK gratefully acknowledges support from the Institute for Advanced Study.

## REFERENCES

- Abbott, B. P., Abbott, R., Abbott, T. D., et al. 2016, *Physical Review Letters*, 116, 061102
- Abbott, B. P., Abbott, R., Abbott, T. D., et al. 2016, *ApJ*, 818, L22
- Abbott, B. P., Abbott, R., Abbott, T. D., et al. 2016, *Physical Review Letters*, 116, 241102
- Belczynski, K., Holz, D. E., Bulik, T., & O’Shaughnessy, R. 2016, *Nature*, 534, 512
- Crowther, P. A. 2007, *ARA&A*, 45, 177
- de Mink, S. E., & Mandel, I. 2016, *MNRAS*, 460, 3545
- Fryer, C. L., Woosley, S. E., & Heger, A. 2001, *ApJ*, 550, 372
- Glebbeek, E., Gaburov, E., de Mink, S. E., Pols, O. R., & Portegies Zwart, S. F. 2009, *A&A*, 497, 255
- Kushnir, D. 2015a, arXiv:1502.03111
- Kushnir, D. 2015b, arXiv:1506.02655
- Kushnir, D., Zaldarriaga, M., Kollmeier, J. A., & Waldman, R. 2016, arXiv:1605.03810
- Loeb, A. 2016, *ApJ*, 819, L21
- Lyman, J. D., Bersier, D., James, P. A., et al. 2016, *MNRAS*, 457, 328
- Mandel, I., & de Mink, S. E. 2016, *MNRAS*, 458, 2634
- Marchant, P., Langer, N., Podsiadlowski, P., Tauris, T. M., & Moriya, T. J. 2016, *A&A*, 588, A50
- McCandliss, S. R., Bohannon, B., Robert, C., & Moffat, A. F. J. 1994, *Ap&SS*, 221, 155
- McClelland, L. A. S., & Eldridge, J. J. 2016, *MNRAS*, 459, 1505
- Morel, T., St-Louis, N., & Marchenko, S. V. 1997, *ApJ*, 482, 470
- Morel, T., Marchenko, S. V., Eenens, P. R. J., et al. 1999, *ApJ*, 518, 428
- Nieuwenhuijzen, H., & de Jager, C. 1990, *A&A*, 231, 134
- Nugis, T., & Lamers, H. J. G. L. M. 2000, *A&A*, 360, 227
- Packet, W. 1981, *A&A*, 102, 17
- Paxton, B., Bildsten, L., Dotter, A., et al. 2011, *ApJS*, 192, 3
- Paxton, B., Cantiello, M., Arras, P., et al. 2013, *ApJS*, 208, 4
- Paxton, B., Marchant, P., Schwab, J., et al. 2015, *ApJS*, 220, 15
- Peters, P. C. 1964, *Physical Review*, 136, 1224
- Perna, R., Lazzati, D., & Giacomazzo, B. 2016, *ApJ*, 821, L18
- Phinney, E. S. 1991, *ApJ*, 380, L17
- Reisswig, C., Ott, C. D., Abdikamalov, E., et al. 2013, *Physical Review Letters*, 111, 151101
- Ro, S., & Matzner, C. D. 2016, *ApJ*, 821, 109
- Schaerer, D., & Maeder, A. 1992, *A&A*, 263, 129
- Schaller, G., Schaerer, D., Meynet, G., & Maeder, A. 1992, *A&AS*, 96, 269
- Sigurdsson, S., & Hernquist, L. 1993, *Nature*, 364, 423
- St-Louis, N., Dalton, M. J., Marchenko, S. V., Moffat, A. F. J., & Willis, A. J. 1995, *ApJ*, 452, L57
- Tutukov, A. V., & Yungelson, L. R. 1993, *MNRAS*, 260, 675

- Vink, J. S., de Koter, A., & Lamers, H. J. G. L. M. 2001, *A&A*, 369, 574  
Woosley, S. E. 2016, *ApJ*, 824, L10  
Yoon, S.-C., Langer, N., & Norman, C. 2006, *A&A*, 460, 199  
Zahn, J.-P. 1975, *A&A*, 41, 329

This paper has been typeset from a  $\text{\TeX}/\text{\LaTeX}$  file prepared by the author.